Clinical and Translational Imaging (2022) 10:587–596
https://doi.org/10.1007/s40336-022-00520-w

MINI-REVIEW

ImmunoPET for prostate cancer in the PSMA era: do we need other targets?

Luca Filippi[1] · Laura Evangelista[2] · Mike M. Sathekge[3,4] · Orazio Schillaci[5,6]

Received: 27 June 2022 / Accepted: 25 July 2022 / Published online: 21 August 2022

Abstract

Introduction In recent years, prostate specific membrane antigen (PSMA) has been gaining a crucial role for prostate cancer (PC) management, representing an ideal platform to combine diagnosis and therapy in a unique approach, namely theranostics. However, low or absent PSMA expression has been reported in up to 20% of PC cases. Our aim was to review the applications of PET/CT with radiolabeled antibodies (immunoPET) to identify biomarkers other than PSMA, potentially suitable for PC theranostics.

Methods We performed a Pubmed/Medline research to identify the most relevant findings of the literature published to date on this topic.

Result Prostate stem cell antigen (PSCA), a biomarker strongly overexpressed in metastatic castration-resistant PC (mCRPC), was effectively imaged in animal models through immunoPET with ^{124}I and ^{89}Zr-conjugated antibody fragments (minibodies) and gave promising results as a theranostic target in preliminary radioimmunotherapeutic applications. Delta-like ligand 3 (DLL3), a molecule associated with PC switching toward neuroendocrine differentiation, was also successfully imaged via immunoPET with ^{89}Zr-labeled antibodies. Other biomarkers, among whom vascular endothelial growth factor receptor 2 (VEGFR-2) and CD46, were also investigated through immunoPET in pre-clinical studies.

Conclusion ImmunoPET pre-clinical studies have identified several biomarkers with potentially high impact on PC theranostics.

Keywords ImmunoPET · Prostate cancer · Precision medicine · Castration-resistant prostate cancer · PET/CT · Theranostics

Introduction

Prostate specific membrane antigen (PSMA) has recently emerged as the "star target" of prostate cancer (PC) imaging through positron emission tomography/computed tomography (PET/CT) and has been successfully applied for PC management [1, 2]. Furthermore, PET/CT with radiolabeled PSMA-ligands (e.g. ^{68} Ga-PSMA-11, ^{18}F-PSMA-1007, etc.…) plays an essential role for the identification of patients, affected by metastatic castration-resistant PC (mCRPC), eligible for PSMA-targeted radioligand therapy, entailing radiopharmaceuticals labeled with beta or alpha-emitters (i.e. ^{177}Lu/^{225}Ac-PSMA-617), therefore combining diagnosis and therapy in a unique approach, namely "theranostics" [3, 4].

However, cases of PSMA-negative PC have been reported, thus supporting the continued value of PET imaging with metabolic tracers, such as ^{18}F/^{11}C-choline [5]. In a recently

✉ Luca Filippi
lucfil@hotmail.com

1 Department of Nuclear Medicine, Santa Maria Goretti Hospital, Via Canova 3, 04100 Latina, Italy

2 Nuclear Medicine Unit, Department of Medicine (DIMED), University of Padua, Via Giustiniani 2, 35128 Padua, Italy

3 Department of Nuclear Medicine, University of Pretoria, Pretoria 0001, South Africa

4 Nuclear Medicine Research Infrastructure (NuMeRI), Steve Biko Academic Hospital, Pretoria 001, South Africa

5 Department of Biomedicine and Prevention, University Tor Vergata, Rome, Italy

6 IRCCS Neuromed, Pozzilli, Italy

published correlative study between ^{68} Ga-PSMA-11 PET/CT and histochemical analysis on post-prostatectomy specimens in 40 patients with therapy- "naïve" PC, a variable grade of heterogeneity of PSMA expression was detected in the majority of patients [6]. One the most plausible explanations for lack of PSMA expression is represented by the deletion of the PSMA-encoding gene (FOLH1) [7], or PC neuroendocrine differentiation (NEPC) [8]. Notably, it has been reported that up to 20% of mCRPC patients present low or absent PSMA expression at PET/CT [9]. Heterogeneity of target expression in disseminated disease represents one of the major causes of PSMA-targeted radioligand therapy failure [10]. This issue is of utmost importance since mCRPC, in spite of recent advances in diagnosis and therapy, still remains a challenging clinical condition, characterized by limited therapeutic options and dismal prognosis [11].

ImmunoPET is a novel imaging approach based on the administration of radiolabeled antibodies, combining the superior diagnostic performance of PET/CT technology with antibodies' high specificity [12]. ImmunoPET has been increasingly applied for the in vivo detection of several tumor-associated biomarkers, showing a particularly relevant impact on patients' stratification prior to molecularly targeted therapies [13].

The aim of this review is to survey the existing literature focused on the applications of immunoPET for the identification of biomarkers alternative to PSMA with potential theranostic impact on PC.

Materials and methods

Electronic literature search on Pubmed/Medline for the English articles, published up to April 2022 on the topic, was performed. Boolean operators (OR, AND) were used to combine the following keywords: "immunoPET", immunoPET", "zirconium-89", "^{89}Zr", "iodine-124, "^{124}I", "prostate cancer", "castration-resistant prostate cancer", "neuroendocrine prostate cancer". No filters other than the languages were applied. The most relevant studies focusing on biomarkers other than PSMA were retrieved, analyzed and discussed. References of the selected manuscripts were also examined for additional relevant studies on the topic. Any discrepancy was resolved by discussion among authors. As this was not a systematic review or meta-analysis, no statistical analysis was performed.

Results

Totally, 10 articles were retrieved by the literature search. The characteristics of the selected studies were reported in Table 1. The main topics were discussed in each following paragraph.

ImmunoPET: basic principles

One of the most peculiar features of molecular imaging through PET/CT or single photon emission tomography (SPECT) is represented by the use of imaging probes capable to investigate physiopathological processes at a cellular and molecular level [14, 15]. In past years immunoscintigraphy, consisting in the administration of antibodies conjugated with gamma-emitting radionuclides (i.e. ^{123}I or ^{99m}Tc), has been applied in oncological and non-oncological field. As specifically concerns PC, interesting results have been obtained by employing ^{111}In- CHX-A"DTPA-trastuzumab to demonstrate and quantify human epidermal growth factor receptor type 2 (HER2) in PC animal models [16, 17]. However, immunoscintigraphy's spreading has been limited by the relatively low spatial resolution of conventional scintigraphy, partially overcome by the implementation of the hybrid SPECT/CT devices [18, 19].

First attempts to develop radioimmunoconjugates suitable for immunoPET have been made by utilizing the positron-emitter iodine-124 (^{124}I) [20]. A cornerstone for the implementation of immunoPET has been represented by the development of antibodies labeled with zirconium-89 (^{89}Zr), a positron emitter characterized by a physical half-life (i.e. 78.4 h) compatible with the slow clearance and long residence of antibodies in the organism after the administration [21]. Furthermore, ^{89}Zr can be easily produced by irradiation of natural yttrium with 13-MeV protons and several commercial suppliers exist to make this nuclide available worldwide. Furthermore, ^{89}Zr can be efficiently bound to antibodies through the bifunctional chelator desferrioxamine (DFO) [22]. Many monoclonal antibodies (MoAbs) have been labeled with ^{89}Zr for immunoPET with satisfying results, among whom trastuzumab, bevacizumab and cetuximab [23–25]. In this regard, the PSMA-targeting humanized MoAb J591, conjugated with ^{89}Zr through DFO, was assessed as a PET molecular probe in a phase I study carried out in 10 patients with histologically proven PC: optimal time for patient imaging after injection resulted in 7 ± 1 days, being liver, renal cortex and bone marrow the critical organs [26]. Of note, 12 lesions in 8 out of the 10 enrolled subjects were submitted to biopsy and confirmed as PC metastatic localizations, 11 of whom were positive at PET/CT examination. The main limitation of ^{89}Zr-DFO-J591 was represented by its slow blood clearance, entailing PET imaging to be performed at a late time (6–8 days after injection) to obtain a satisfying tumor-to-background ratio. To overcome these drawbacks, IAB2M, an 80-kDa minibody genetically engineered from the parent antibody J591 and characterized by a faster blood clearence, was tested as a potential imaging probe

Table 1 Main manuscripts focusing on immunoPET targeting prostate cancer-associated biomarkers

Authors. (ref)	Year of publication	Biomarker	Molecular probes	Setting	Comments
Korsen et al. [46]	2022	DLL3	^{89}Zr-DFO-SC16 *vs* ^{68} Ga-PSMA-11 or ^{68} Ga-DOTATATE	Identification of DLL3, a surrogate biomarker of neuroendocrine differentiation of prostate cancer	ImmunoPET effectively identified DLL3 + xenografts in mice, while tumors were not detected by both ^{68} Ga-PSMA-11 and ^{68} Ga-DOTATATE
Arndt et al. [41]	2022	PSCA	^{64}Cu-TM	Development of a multimodality platform both for CAR T cell therapy and imaging	ImmunoPET with ^{64}Cu-TM efficiently detected PSCA + cells in mice bearing xenografts; CAR T cell therapy targeting PSCA exerted anti-tumor activity in animal models
Wang et al. [51]	2021	CD46	^{89}Zr-DFO-YS5	In vivo imaging of CD46 expression in PC tumors	ImmunoPET with ^{89}Zr-DFO-YS5 clearly detected CD46 expression in mice bearing PC xenografts. In patient-derived xenografts, particularly high uptake was registered in neuroendrocrine tumors
Zettlitz et al. [35]	2020	PSCA	^{124}I-A11 minibody ^{89}Zr-A2 cys-diabody	Comparison of 2 different radiocompounds (^{124}I-labeled *vs* ^{89}Zr-labeled) for immunoPET in PSCA + tumors	In mice genetically modified to mimic physiological human PSCA expression in stomach, bladder and prostate, ^{89}Zr-A2 cys-diabody presented more favorable clearance for immunoPET with respect to ^{124}I-A11 minibody
Tsai et al. [36]	2020	PSCA	ImmunoPET: ^{124}I-A11 Mb ^{89}Zr-DFO-A11 Mb Radioimmunotherapy: ^{131}I-A11 Mb ^{177}Lu-DTPA-A11 Mb	Identification through immunoPET of the most adequate radiolabeled antibodies for RIT application	At immunoPET, ^{124}I-A11 Mb presented the most favorable pharmacokinetic biodistribution for RIT applications. ^{131}I-A11 Mb administration resulted in effective anti-tumor effects in mice bearing PSCA + xenografts
Li et al. [49]	2019	VEGFR-2	^{89}Zr-Df-R	Use of immunoPET for the in vivo assessment of VEGFR expression in PC xenografts	ImmunoPET with ^{89}Zr-Df-R effectively visualized VEGFR-2 expression in mice bearing xenografts, with higher tracer uptake in PC3 cell lines showing the highest VEGFR-2 levels a flow cytometry
Tsai et al. [33]	2018	PSCA	^{124}I-A11 minibody ^{89}Zr-A11 cMb-Cy5.5	Dual-imaging modality through immunoPET and fluorescence to optimize tumor margin delineation	The combined use of immunoPET and fluorescence resulted useful to optimize tumor margin delineation in mice intraprostatic implant, thus being of potential usefulness for near-infrared fluorescence (NIRF)-guided surgery
van Rij et a. [54]	2015	TROP-2	^{68} Ga-IMP288 *vs* [^{18}F]FDG	Pre-targeting immunoPET for the detection of TROP-2 expression in PC3 xenografts	ImmunoPET through pre-targeting effectively detected TROP-2 expression in mice bearing PC3 xenografts as early as 1 h p.i. and outperformed [^{18}F]FDG PET for the visualization of both lesions in mice flank and peritoneum
Knowles et al. [31]	2014	PSCA	^{124}I-A11 minibody ^{89}Zr-A11 minibody	Imaging of mice bearing PSCA + tumors	Both ^{124}I and ^{89}Zr-minibodies efficiently imaged PSCA-expressing xenografts, but ^{124}I-labeled compounds showed higher imaging contrast
Knowles et al. [32]	2014	PSCA	^{124}I-A11 minibody	Comparison between immunoPET and PET with ^{18}F-NaF in mice with bone tumors	ImmunoPET showed superior diagnostic performance with respect to ^{18}F-NaF for detecting PSCA-positive bone metastases and resulted an effective tool for monitoring response to anti-androgen therapy

to target PSMA extracellular domain [27]. In a phase I/IIa study ^{89}Zr-labeled IAB2M (^{89}Zr-DFO-IAB2M) resulted effective for the detection of PC metastases to bone and lymph nodes in 17 patients through PET/CT scan as early as at 24 and 48 h post tracer administration [28]. On this path, Frigerio et al. investigated the PSMA-directed scFvD2B antibody fragment as an imaging probe for PC in animals models by labeling it with ^{124}I. ^{124}I-scFvD2B was intensely incorporated in PSMA-positive cells and allowed the in vivo detection of PSMA-positive tumors at 15 and 24 h, while it showed not meaningful accumulation in animals with PSMA-negative lesions [29].

Notably, immunoPET has emerged as an essential tool for the development of antibody–drug conjugates (ADCs), not only to image and quantify target-specific drug accumulation but also to study drug-biokinetics through serial PET/CT acquisitions at different time-intervals [30]. This issue is of foremost importance when ADCs' effectiveness is enhanced by labeling with a beta or alpha emitter to perform radioimmunotherapy (RIT) [31]. However, it has to be underlined that, although it is extremely promising, several issues remain to be addressed to improve ^{89}Zr-immunoPET: such as the binding stability of DFO chelator and several technical factors concerning PET/CT image quality and accuracy of quantification [32].

Prostate stem cell antigen

Prostate stem cell antigen (PSCA) is a small, glycosylphosphatidylinositol (GPI)-anchored cell surface protein, characterized by a 30% of homology with stem cell antigen type 2 (SCA-2), a surface biomarker of immature lymphocyte [33]. In spite of its denomination, PSCA is mainly expressed by differentiated cells and strongly overexpressed in PC; notably, PSCA density in tumor tissue correlated with adverse prognostic factors such as high Gleason score and propensity to metastatization [34]. Although it has been hypothesized that PSCA function is linked with mechanisms involving cell adhesion and migration, its exact role remains unclear and, as matter of fact, PSCA-knockout mice did not show relevant abnormalities [35].

PSCA has several characteristics that make it a potentially useful biomarker for immunoPET and theranostics in mCRPC: firstly, it is located on cell surface, therefore being exposed to extracellular space and circulating ligands. Secondly, increased PSCA level expression has been found associated with PC transition toward castration-resistant state [36].

One of the first efforts to develop radiolabeled antibodies for PSCA-targeted immunoPET has been carried out by Knowles et al. [37]. The authors synthesized an anti-PSCA minibody, an engineered 80 kDa antibody fragment (scFv-CH3 homodimer), suitable for conjugation both with ^{124}I and ^{89}Zr (i.e. A11 anti-PSCA minibody). Both ^{124}I- and ^{89}Zr-labeled minibodies were tested for PET-imaging in mice bearing PSCA-positive xenografts. The authors found rapid and specific incorporation of both ^{124}I and ^{89}Zr-labeled minibodies in PSCA-positive xenografts: ^{124}I-labeled minibodies presented high imaging contrast thanks to the lower non-specific uptake in soft tissues, therefore showing the most favorable characteristics to be implemented as an imaging agent. On the path of these encouraging results, the same group of research further investigated the potential of anti-PSCA ^{124}I-labeled minibodies for the imaging of PC disease progression and response to therapy in animal models [38]. SCID male mice were implanted with LAPC-9 xenografts in the subcutaneous tissues and were also injected in the proximal tibia with PSCA-positive tumor cells (control group received PSCA-negative cells). Mice bearing intratibial tumors were submitted to PET/CT with ^{18}F-fluoride (^{18}F-NaF), which is generally considered the most comprehensive imaging modality to assess metastatic bone disease. Immediately after ^{18}F-NaF PET/CT or the day after, mice were administered with ^{124}I-labeled minibodies and were then imaged with microPET at 44 h after tracer administration. Both ^{18}F-NaF PET/CT and immunoPET images were repeated at different time-points and evaluated both qualitatively and quantitatively, by calculating the grade of tracer uptake as %ID/g. While bone scan through ^{18}F-NaF showed a considerable amount of non-specific uptake hampering the detection of tibial tumor implant at the different time-points, immunoPET with ^{124}I-labeled anti-PSCA minibodies demonstrated increased tracer incorporation in tibial tumor in 67% of mice at 4 weeks and in 100% of mice at 6 and 8 weeks after implantation. Furthermore, the authors used immunoPET for monitoring changes in PSCA expression in mice bearing LAPC-9 xenografts, divided in 2 groups: the former submitted to anti-androgen therapy with MDV-3100 (enzalutamide) and the latter treated with vehicle (i.e. water with 1% carboxymethylcellulose): ^{124}I-labeled minibodies uptake and tumor volumes were comparable among the 2 groups before starting the different treatments. After 1 week of therapy, tumor volumes were not significantly changed among the 2 groups on CT scan, on the contrary ^{124}I-labeled minibody uptake was substantially lower in mice treated with MDV-3100 with respect to the vehicle group. The data were in accordance with cytometry performed on LAPC-9 digested cells showing that MDV-3100 treatment led to a downregulation of PSCA expression (i.e. $62.8 \pm 4.9\%$ reduction). In light of the above, the authors suggested that ^{124}I-labeled minibodies might represent useful imaging agent for the in vivo monitoring of PSCA-expression in CRPC during 2nd generation anti-androgen therapy.

Tsai and collaborators investigated the possible application of PSCA as a target for imaging and near-infrared fluorescence (NIRF)-guided surgery [39]. NIRF-guided surgery

consists in the utilization of specific dyes to improve surgical margin delineation and has been applied with encouraging results in uro-oncology, especially in robotic-assisted procedures [40]. To obtain a molecular probe suitable both for NIRF and immunoPET, Tsai's group synthesized a cysteine-modified humanized anti-PSCA A11 Mb (A11 cMb), that was site-specifically conjugated with the near-infrared fluorophore Cy5.5 and was also radiolabeled with ^{124}I or ^{89}Zr. ^{124}I-A11 cMb-Cy5.5 was utilized for immunoPET/fluorescence in nude mice bearing xenografts expressing moderate or high PSCA levels, while ^{89}Zr-A11 cMb-Cy5.5 was applied as a dual-modality imaging in mice bearing orthotopic tumors. Of note, the authors found ^{124}I-immunoPET/fluorescence capable to effectively image PSCA-expressing cells, with high imaging contrast, in xenografted mice, as confirmed also by ex vivo analysis. On its turn, ^{89}Zr-immunoPET/fluorescence was effective for the detection of intraprostatic implanted PSCA-positive cells, while fluorescence imaging clearly discriminated intraprostatic tumor margins with respect to neighboring seminal vesicles.

Zettlitz et al. further explored the potential of PSCA-targeting antibodies in a human prostate stem cell antigen knock-in (hPSCA KI) mouse model [41]. In hPSCA KI mice PSCA was expressed, as it physiologically occurs in humans, in stomach, bladder and prostate gland. The authors' aim was to assess whether PSCA physiological signal might hamper the detection of PSCA-positive tumors through immunoPET. They utilized either ^{124}I-labeled anti-PSCA minibodies or ^{89}Zr-conjugated A2 cys-diabodies. After i.v. administration, ^{124}I-labeled minibodies efficiently revealed physiological activity in stomach, bladder and prostate in hPSCA KI mice, but due to their molecular weight (i.e. 80 kDa), non-specific blood activity remained high up to 20 h post-injection. On the contrary, ^{89}Zr-A2 cys-diabodies showed faster clearance thanks to their lower weight (i.e. 50 kDa) and efficiently detected PSCA-positive xenografts mice.

As far as it concerns the theranostic counterpart of PSCA-targeting approaches, possible RIT applications in animal models were investigated by Tsai and colleagues by labeling A11 minibodies with 2 distinct beta-emitters: iodine-131 (^{131}I), characterized by a $t_{1/2} = 8.0$ days and E(max) = 606 keV, and luthetium-177 (^{177}Lu), exhibiting a $t_{1/2} = 6.7$ days and E(max) = 497 keV [42]. In a first phase, immunoPET with either ^{124}I-A11 Mb or ^{89}Zr-DFO-A11 Mb was utilized to profile the pharmacokinetic characteristics of ^{131}I-A11 Mb and ^{177}Lu-DTPA-A11 Mb in animal models. After having identified ^{131}I-A11 Mb as the best candidate for RIT due to its lower blood pool and soft tissue activity, RIT through escalating single doses (3.7, 11 or 37 MBq) and saline control was administered to 2 groups of mice bearing PSCA-positive tumors, while toxicity was tested in hPSCA KI mice. The authors monitored mice both for RIT anti-tumor effectiveness (change in tumor volume) and toxicity (change in mice weight). RIT with anti-PSCA ^{131}I-A11 Mb through single dose approaches presented a dose-dependent anti-tumor activity, with minimal off-target toxicity, and resulted effective to improve median survival in treated mice with respect to the control group.

Immunotherapy, consisting of unleashing host immune system against tumor is a therapeutic approach that has gained a central role in oncology through the introduction of immune checkpoint inhibitors (ICIs) and chimeric antigen receptor (CAR)-T cell therapy [43, 44]. In particular, it has to be underlined that CAR-T cell therapy can be associated with some severe adverse effects, such as cytokine release syndrome (CRS), CAR T-cell–related encephalopathy syndrome (CRES) or immune effector cell–associated neurotoxicity syndrome (ICANS) [45]. To promptly manage potential adverse effects associated with CAR-T cell therapy, several efforts have been made to develop a switchable platform, namely "UniCAR", suitable for redirecting immune system from an active state to an inactive one. UniCAR-T cells are activated by binding to a specific target module (TM) which works as a "bridge" between T cells and a tumor-associated biomarker. Therefore, while infusion of TM to the patient leads UniCAR T cells to the "ON" mode, when the TM is physiologically removed from the organism, cells come back to the "OFF" mode [46]. In this way, CAR-T cell's activity can be controlled and modulated by clinicians. In this perspective, Arndt and colleagues have recently developed a flexible approach for a PSCA-targeted immunoPET and RIT by utilizing UniCAR platform [47]. The authors synthesized a novel IgG4-based TM targeting PSCA: immunodeficient mice were subcutaneously injected with PC3 tumors (positive for PSCA/PSMA/luciferase) alone or in combination with UniCAR T cells (i.e. luciferase was utilized to monitor tumor growth through bioluminescence). In mice infused with anti-PSCA IgG4-based TM, UniCAR T cells were activated and efficiently exerted anti-tumor activity, as demonstrated by bioluminescence analysis, while no anti-tumor activity was detected in mice that did not receive TM. A further endpoint of the cited study consisted of entailing the IgG4-based TM for theranostic purposes, by labeling it through a bifunctional chelator (DOTAGA) with the positron-emitter copper 64 (^{64}Cu) for the imaging and with the alpha emitter actinium-225 (^{225}Ac) for therapy, respectively. As far as it concerns the imaging phase, ^{64}Cu-TM was tested in mice bearing PSCA-positive xenografts and, after administration, the radiocompound rapidly cleared from blood and was promptly incorporated within tumors. Of note, at later time-points of imaging, ^{64}Cu-TM's distribution included heart, liver, kidneys, with no evidence of uptake in salivary glands. For the therapeutic part of the study, mice bearing PSCA-positive tumors were divided in 2 groups and administered, alternatively, with ^{225}Ac-TM (5 kBq per animal; approximately 200 kBq/kg) or DOTAGA-TM (i.e.

controls): at day 43 post therapy, tumor growth was significantly reduced in the ^{225}Ac-TM treated mice with respect to controls. At the administered activity, no relevant adverse effects were registered.

Delta-like ligand 3 (DLL3)

Lineage switching represents one of most crucial features involved in tumor resistance to therapy and consists in the capability of a single genotype to generate often radically different alternative phenotypes as a response to changes in the cell environment [48]. By redirecting their phenotype to a state capable to proliferate independently from a certain metabolic pathway molecularly targeted by therapy, tumors can become "therapy-resistant". As specifically regards PC, prolonged inhibition of the androgen axis through ADT or 2nd generation anti-androgens may lead cells to lineage switching toward neuroendocrine differentiation [49], giving rise to the so-called treatment-induced NEPC. Several similarities have been reported among NEPC and small cell lung cancer (SCLC), such as the aggressive behavior and, from a molecular point of view, the suppression of Notch signaling activity through the upregulation of the inhibitory Notch ligand delta-like ligand 3 (DLL3) [50]. As a matter of fact, DDL3 has been found overexpressed in the majority of NEPC samples, while it is absent or minimally detectable in non-malignant cells. These characteristics make DLL3 a potentially useful biomarker for theranostic applications in NEPC.

In this perspective, a DLL3-targeted humanized MoAb–SC16 was developed and chemically modified to be labeled with ^{89}Zr through DFO by Sharma and colleagues [51] to allow an in vivo assessment of DLL3 expression in SCLC models. In a very recently published paper [52], Korsen and co-workers applied immunohistochemistry and qPCR to gage androgen receptor-associated biomarkers and NEPC-associated biomarkers in a panel of PC cell lines. They identified a peculiar cell line, namely H660, as positive for DLL3 and negative for androgen-associated biomarkers (PSA, PSMA) both at a transcriptional and translational level. Subsequently, mice bearing both DLL3-positive (cell line: H660) and DLL3-negative (cell line: DU145) xenografts were submitted to DLL3-targeted PET-imaging with ^{89}Zr-DFO-SC16: tracer incorporation was rapid and intense in H660 xenografts, with increasing uptake value over time (i.e. maximum uptake reached at 120 h post-injection). On the contrary, minimal uptake of ^{89}Zr-DFO-SC16 was evident in DU145 xenografts. Notably, another group of male mice was subcutaneously injected with both LNCaP (PSMA-positive/DLL3-negative) and H660 (PSMA-negative/DLL3-positive) xenografts on the opposite flanks and then submitted to ^{68} Ga-PSMA-11 PET/CT: at 1 h after administration only LNCaP xenografts presented high ^{68} Ga-PSMA-11 incorporation. Two days later, the same group of mice underwent ^{89}Zr-DFO-SC16 immunoPET that effectively imaged H660 xenografts while no meaningful uptake was registered in LNCaP tumors. Notably, H660 xenografts were negative also when examined with ^{68} Ga-DOTATATE, which is currently applied in clinical practice to detect somatostatin-receptor expression, indicative of neuroendocrine differentiation in tumors [53, 54].

Vascular endothelial growth factor receptor 2 (VEGFR-2)

Vascular endothelial growth factor receptor 2 (VEGFR-2) is a tyrosine kinase receptor for the angiogenic growth factor, VEGF, that, in its turn, encompasses a family of growth factors including several members (i.e. VEGF-A, -B, -C and –D). VEGFR-2 preferentially binds to VEGF-A triggering a complex signaling cascade involving secondary messengers including several protein kinases and phosphatases, leading to cell proliferation and supporting the so-called "proangiogenic phenotype" [55]. Since VEGF/VEGFR expression was found upregulated in PC and associated with tumor stage, aggressiveness, propensity to colonize bone, several efforts have been made to develop an immunoPET platform targeting VEGFR [56].

Li and co-workers conjugated ramucirumab, a recombinant humanized IgG1 monoclonal antibody, with ^{89}Zr through the chelator DFO (^{89}Zr-Df-R) and tested this radiocompound as an imaging probe for the in vivo assessment of VEGFR-2 expression in mice bearing subcutaneous xenografts of different PC lines [57]. Expression of VEGFR-2 was gaged in 3 PC cell lines (i.e. PC3, LNCaP and LAPC-4) through flow cytometry: among the analyzed cells, PC3 presented the highest VEGFR-2 levels. After having subcutaneously injected tumor cells of the 3 different lines to mice, immunoPET with ^{89}Zr-Df-R was carried out to visualize VEGFR-2 expression in xenografts by acquiring images at different time-points. ImmunoPET showed intense tracer incorporation in PC3 xenografts, according to the high levels of VEGFR-2 detected by flow cytometry in these tumor cells, with a peak of uptake reached at 96 h post-injection. On the contrary, only mild tracer uptake was revealed in LNCaP and LAPC-4 xenografts, consistently with a lower VEGFR-2 density demonstrated at cytometry. Notably, ^{89}Zr-Df-R incorporation in PC3 xenografts resulted significantly reduced by administering "cold" ramucirumab, thus indicating the specificity of tracer binding to VEGFR-2. The authors also performed a biodistribution study that showed similar patterns of tracer's distribution in mice bearing the 3 distinct types of xenografts, being spleen, liver and blood the major sites of radiocompound's aspecific uptake. In spite of these promising results, to the best of our knowledge no further investigations were performed on

VEGFR-2 as potentially useful biomarker for PC diagnosis and theranostics.

CD46

Human membrane co-factor protein, namely CD46, plays a central role as negative regulator of the complement cascade in the innate immune system and protects autologous cells from complement attack by binding to some complement factors such as C3b and C4b.

CD46 extracellular domain consists of short consensus repeats (SCR1-SCR4) forming an elongated structure [58]. Of note, CD46 was found overexpressed in localized and metastatic PC (both in adenocarcinoma and NEPC), while it is only minimally detectable on normal tissue and, most interestingly, CD46 expression resulted enhanced in mCRPC after treatment with abiraterone and enzalutamide [49].

A CD46-targeted immunoPET resulted feasible thanks to the development of YS5, a human full-length IgG1, radiolabeled with ^{89}Zr (^{89}Zr-DFO-YS5), synthesized by Wang et al. [59]. ImmunoPET with ^{89}Zr-DFO-YS5 was performed in mice bearing 2 distinct types of tumors, DU145 (AR/PSMA-negative, CD46-positive) and 22Rv1 (AR/CD46/PSMA-positive), through repeated acquisitions up to 168 h after tracer administration; furthermore, mice bearing tumors were sacrificed at different time points for biodistribution studies. In PSMA-negative/CD46-positive xenografts (DU145), tracer uptake reached the highest value (i.e. 18.2 ± 10.9%ID/gram) at 168 h and the greatest tumor/muscle ratio (i.e. 59.0 ± 16.5) at 96 h.

Interestingly, in mice bearing PSMA/CD46-positive tumors (22Rv1), the biodistribution of ^{89}Zr-DFO-YS5 was compared with that of ^{68} Ga-PSMA-11: ^{89}Zr-DFO-YS5 presented high uptake in tumor but all the other organs had an uptake value below 5% at 4 day p.i., while ^{68} Ga-PSMA-11 uptake measured at 1 h p.i. resulted remarkably high both in tumor and kidneys. It is worth mentioning that imaging with ^{89}Zr-DFO-YS5 was also tested by the authors in mice bearing several patient-derived xenografts: CD46 was clearly detected by immunoPET, especially in case of LTL-545 neuroendocrine prostate cancer tumors.

Trophoblast cell surface antigen 2 (TROP-2)

Trophoblast cell surface antigen 2 (TROP-2), firstly described as a protein highly expressed on the surface of trophoblast cells, is a 46-kDa transmembrane glycoprotein, only minimally detectable in normal glandular cells, while it has been found overexpressed in several tumors such as bladder, lung, breast and gastric cancer [60]. As specifically regards PC, TROP-2 has been found significantly elevated in CRPC and NEPC [61].

An interesting strategy for the in vivo imaging of TROP-2 expression in PC through immunoPET has been developed by van Rij and co-workers [62]. To obtain an optimal tumor-to-background ratio, a pre-targeting approach was employed via a bispecific monoclonal antibody (bsmAb), TF12, presenting 2 sites binding to TROP-2 (i.e. anti-TROP-2 Fab fragments) and 1 site targeting HSG (histamine-succinyl-glycine). In the pre-targeting approach, TF-12 is firstly intravenously administered; subsequently, after that the amount of TF-12 not bound to tumor has cleared from blood, the HSG-substituted radiolabeled hapten-peptide is injected and rapidly incorporated into the tumor by the anti-HSG arm of the bsmAb [63]. Nude mice were injected with PC3 cells in the flank or in the peritoneum to test anti-TROP-2 immunoPET: ^{18}F-fluorodeoxyglucose ([^{18}F]FDG) was used as a reference. Therefore, each mouse was submitted both to PET/CT with [^{18}F]FDG and anti-TROP-2 immunoPET. For immunoPET, pre-targeting was carried out through the administration of TF-12 followed, after 16 h, by the injection of a HSG-substituted radiolabeled hapten-peptide, namely ^{68} Ga-IMP288: PET/CT was performed 1 h after labeled hapten administration. After 48 h, the same animal was administered with [^{18}F]FDG and submitted to PET/CT at 45 min post-injection. It is worth mentioning that pre-targeting allowed obtaining an excellent tumor-to-blood ratio in all mice bearing PC3 xenografts as early as 1 h after injection. Of note, immunoPET with ^{68} Ga-IMP288 outperformed PET with [^{18}F]FDG for the visualization of xenografts both in mice flank and peritoneum, being effective to identify lesions as small as 5 mm^3.

Concluding remarks and future directions

ImmunoPET was successfully employed for the investigation of several biomarkers, other than PSMA, that might have a great impact on PC theranostics. However, existing literature on this topic is still limited to pre-clinical studies, since none of the aforementioned molecular targets has been evaluated in humans yet. Notably, one of the most relevant issues limiting the diffusion of immunoPET is represented by the potential immunogenicity of the different radioimmunoconjugated compounds. However, while murine antibodies obtained from mouse hybridoma were found to elicit meaningful anti-murine antibody (HAMA) response in patients, technological development has recently allowed the production of "humanized" or fully human antibodies, thus minimizing the issues linked to immunogenicity and HAMA production [64].

It has to be underlined that the majority of the studies reported in this review (6 out of 10 papers, 60%) was focused on PSCA, that has been found extremely promising and investigated in several settings (i.e. NIRF-guided surgery, RIT, UniCAR T cell therapy), as schematically

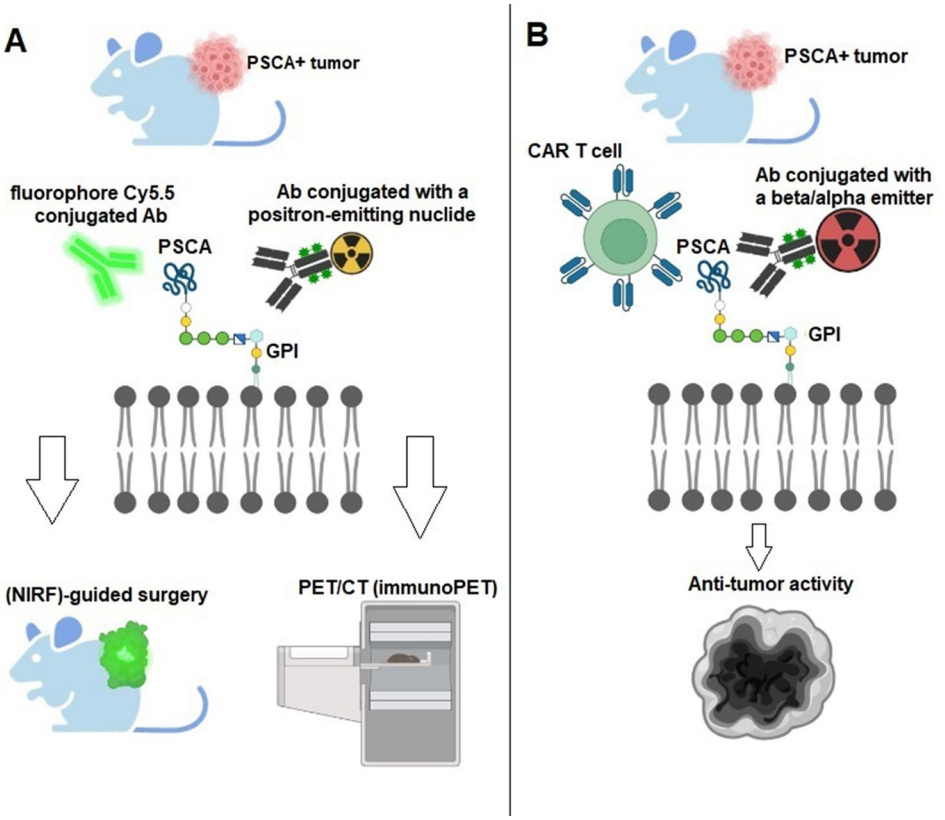

Fig. 1 Schematization of PSCA-targeted theranostic approaches in preclinical studies. On the left side (**A**), applications for imaging are presented, involving engineered antibodies (minibodies) conjugated both with fluorophore for (NIRF)-guided surgery or labeled with positron-emitters (^{124}I, ^{89}Zr, ^{64}Cu) for immunoPET. On the right side (**B**), potential therapeutic applications are illustrated: PSCA-targeted CAT T cells or antibodies labeled with beta or alpha particles are administered to obtain anti-tumor effect. Note, at the center of both sections (**A**, **B**), the representation of PSCA structure with its glycosylphosphatidylinositol (GPI)-anchor to the cell membrane (figure created with BioRender.com)

represented in Fig. 1. In particular, in recent years the complex interactions among the various cell types in the tumor microenvironment have emerged as a relevant hallmark of cancer, leading to the design of powerful T-cell therapies that are capable of causing the regression of large tumor burdens [65]. In this regard, it is worth mentioning the ongoing clinical trial (NCT03873805) addressing the impact of PSCA-chimeric antigen receptor (CAR) T cells in patients with PSCA-positive mCRPC. A further interesting clinical trial (NCT04702737) is underway to assess the potential of tarlatamab (AMG 757), a half-life extended bispecific T-cell engager, as a therapeutic tool in DDL3-positive NEPC cells. In the aforementioned clinical trials, target identification (PSCA or DDL3) was based on laboratory findings (histochemistry, genomic analysis). Nevertheless, biopsy represents an invasive approach, not suitable for exploring heterogeneity of target expression in case of multiple localizations.

In this perspective, immunoPET holds the promise to become an essential tool for a patient-tailored approach in PC, being suitable for an in vivo assessment and quantification of several targets alternative to PSMA, according to tumor biology and evolution, and allowing dynamic evaluation of eventual changes in biomarkers' expression during therapy.

Acknowledgements Not applicable.

Author contributions All the authors equally contributed to conception and design of the article, or acquisition, analysis and interpretation of data; L.F. and L.E. wrote the initial draft of the manuscript; M.M.S. and O.S. critically revised the manuscript for important intellectual content.

Funding No funding was received.

Availability of data and material Not applicable.

Declarations

Competing interests The authors declare that they have no competing interest.

Ethics approval and consent to participate Not applicable.

Consent for publication Not applicable.

References

1. Evangelista L, Maurer T, van der Poel H et al (2022) [68Ga] Ga-PSMA versus [18F]PSMA positron emission tomography/computed tomography in the staging of primary and recurrent prostate cancer. a systematic review of the literature. Eur Urol Oncol 5:273–282. https://doi.org/10.1016/j.euo.2022.03.004
2. Mei R, Farolfi A, Morigi JJ, Fanti S (2022) The role of prostate-specific membrane antigen PET/computed tomography in the management of prostate cancer patients: could we ask for more?

Curr Opin Urol 32:269–276. https://doi.org/10.1097/MOU.0000000000000982
3. Mokoala K, Lawal I, Lengana T et al (2021) PSMA theranostics: science and practice. Cancers 13:3904. https://doi.org/10.3390/cancers13153904
4. Filippi L, Chiaravalloti A, Schillaci O, Bagni O (2020) The potential of PSMA-targeted alpha therapy in the management of prostate cancer. Expert Rev Anticancer Ther 20:823–829. https://doi.org/10.1080/14737140.2020.1814151
5. Alberts I, Sachpekidis C, Fech V et al (2020) PSMA-negative prostate cancer and the continued value of choline-PET/CT. Nuklearmedizin 59:33–34. https://doi.org/10.1055/a-1044-1855
6. Cytawa W, Kircher S, Kübler H et al (2022) Diverse PSMA expression in primary prostate cancer: reason for negative [68Ga]Ga-PSMA PET/CT scans? Immunohistochemical validation in 40 surgical specimens. Eur J Nucl Med Mol Imagin. https://doi.org/10.1007/s00259-022-05831-8
7. Maraj B, Markham A (1999) Prostate-specific membrane antigen (FOLH1): recent advances in characterising this putative prostate cancer gene. Prostate Cancer Prostatic Dis 2:180–185. https://doi.org/10.1038/sj.pcan.4500325
8. Bakht MK, Derecichei I, Li Y et al (2019) Neuroendocrine differentiation of prostate cancer leads to PSMA suppression. Endocr Relat Cancer 26:131–146. https://doi.org/10.1530/ERC-18-0226
9. Emmett L, Willowson K, Violet J et al (2017) Lutetium ^{177} PSMA radionuclide therapy for men with prostate cancer: a review of the current literature and discussion of practical aspects of therapy. J Med Radiat Sci 64:52–60. https://doi.org/10.1002/jmrs.227
10. Sgouros G, Dewaraja YK, Escorcia F et al (2021) Tumor response to radiopharmaceutical therapies: the knowns and the unknowns. J Nucl Med 62:12S-22S. https://doi.org/10.2967/jnumed.121.262750
11. Gillessen S, Armstrong A, Attard G et al (2022) Management of patients with advanced prostate cancer: report from the advanced prostate cancer consensus conference 2021. Eur Urol 82:115–141. https://doi.org/10.1016/j.eururo.2022.04.002
12. Wei W, Rosenkrans ZT, Liu J et al (2020) ImmunoPET: concept, design, and applications. Chem Rev 120:3787–3851. https://doi.org/10.1021/acs.chemrev.9b00738
13. Pool M, Kol A, de Jong S et al (2017) ^{89} Zr-mAb3481 PET for HER3 tumor status assessment during lapatinib treatment. mAbs 9:1370–1378. https://doi.org/10.1080/19420862.2017.1371382
14. Stoddart A (2016) Molecular imaging: seeing the target. Nat Rev Mater 1:16057. https://doi.org/10.1038/natrevmats.2016.57
15. Filippi L, Valentini FB, Gossetti B et al (2005) Intraoperative gamma probe detection of head and neck paragangliomas with ^{111} in-pentetreotide: a pilot study. Tumori 91:173–176. https://doi.org/10.1177/030089160509100213
16. Malmberg J, Tolmachev V, Orlova A (2011) Imaging agents for in vivo molecular profiling of disseminated prostate cancer: cellular processing of [111In]-labeled CHX-A″DTPA-trastuzumab and anti-HER2 ABY-025 Affibody in prostate cancer cell lines. Exp Ther Med 2:523–528. https://doi.org/10.3892/etm.2011.217
17. Mendoza N, Phillips GL, Silva J et al (2002) Inhibition of ligand-mediated HER2 activation in androgen-independent prostate cancer. Cancer Res 62:5485–5488
18. Potamianos S, Varvarigou AD, Archimandritis SC (2000) Radioimmunoscintigraphy and radioimmunotherapy in cancer: principles and application. Anticancer Res 20:925–948
19. Filippi L, Schillaci O (2006) SPECT/CT with a hybrid camera: a new imaging modality for the functional anatomical mapping of infections. Expert Rev Med Devices 3:699–703. https://doi.org/10.1586/17434440.3.6.699
20. Chacko A-M, Li C, Nayak M et al (2014) Development of ^{124} I Immuno-PET Targeting Tumor Vascular TEM1/Endosialin. J Nucl Med 55:500–507. https://doi.org/10.2967/jnumed.113.121905
21. van Dongen GAMS, Beaino W, Windhorst AD et al (2021) The role of ^{89} Zr-Immuno-PET in navigating and derisking the development of biopharmaceuticals. J Nucl Med 62:438–445. https://doi.org/10.2967/jnumed.119.239558
22. Yoon J-K, Park B-N, Ryu E-K et al (2020) Current perspectives on 89Zr-PET imaging. IJMS 21:4309. https://doi.org/10.3390/ijms21124309
23. Dijkers ECF, Kosterink JGW, Rademaker AP et al (2009) Development and characterization of clinical-grade ^{89} Zr-Trastuzumab for HER2/ *neu* ImmunoPET imaging. J Nucl Med 50:974–981. https://doi.org/10.2967/jnumed.108.060392
24. Oosting SF, van Asselt SJ, Brouwers AH et al (2016) ^{89} Zr-bevacizumab PET visualizes disease manifestations in patients with von hippel-lindau disease. J Nucl Med 57:1244–1250. https://doi.org/10.2967/jnumed.115.167643
25. Makris NE, Boellaard R, van Lingen A et al (2015) PET/CT-derived whole-body and bone marrow dosimetry of ^{89} Zr-Cetuximab. J Nucl Med 56:249–254. https://doi.org/10.2967/jnumed.114.147819
26. Pandit-Taskar N, O'Donoghue JA, Beylergil V et al (2014) 89Zr-huJ591 immuno-PET imaging in patients with advanced metastatic prostate cancer. Eur J Nucl Med Mol Imag 41:2093–2105. https://doi.org/10.1007/s00259-014-2830-7
27. Pandit-Taskar N, O'Donoghue JA, Ruan S et al (2016) First-in-human imaging with ^{89} Zr-Df-IAB2M anti-psma minibody in patients with metastatic prostate cancer: pharmacokinetics, biodistribution, dosimetry, and lesion uptake. J Nucl Med 57:1858–1864. https://doi.org/10.2967/jnumed.116.176206
28. Joraku A, Hatano K, Kawai K et al (2019) Phase I/IIa PET imaging study with 89zirconium labeled anti-PSMA minibody for urological malignancies. Ann Nucl Med 33:119–127. https://doi.org/10.1007/s12149-018-1312-6
29. Frigerio B, Morlino S, Luison E et al (2019) Anti-PSMA 124I-scFvD2B as a new immuno-PET tool for prostate cancer: preclinical proof of principle. J Exp Clin Cancer Res 38:326. https://doi.org/10.1186/s13046-019-1325-6
30. Carmon KS, Azhdarinia A (2018) Application of immuno-PET in antibody-drug conjugate development. Mol Imag 17:153601211880122. https://doi.org/10.1177/1536012118801223
31. Verel I, Visser GWM, van Dongen GA (2005) The promise of immuno-PET in radioimmunotherapy. J Nucl Med 46(Suppl 1):164S-S171
32. Tateishi U, Daisaki H, Tsuchiya J et al (2021) Image quality and quantification accuracy dependence on patient body mass in 89Zr PET/CT imaging. EJNMMI Phys 8:72. https://doi.org/10.1186/s40658-021-00420-4
33. Saeki N, Gu J, Yoshida T, Wu X (2010) Prostate stem cell antigen: a jekyll and hyde molecule? Fig. 1. Clin Cancer Res 16:3533–3538. https://doi.org/10.1158/1078-0432.CCR-09-3169
34. Han K-R, Seligson DB, Liu X et al (2004) Prostate stem cell antigen expression is associated with gleason score, seminal vesicle invasion and capsular invasion in prostate cancer. J Urol 171:1117–1121. https://doi.org/10.1097/01.ju.0000109982.60619.93
35. Moore ML, Teitell MA, Kim Y et al (2008) Deletion of PSCA increases metastasis of TRAMP-Induced prostate tumors without altering primary tumor formation. Prostate 68:139–151. https://doi.org/10.1002/pros.20686
36. Gu Z, Thomas G, Yamashiro J et al (2000) Prostate stem cell antigen (PSCA) expression increases with high gleason score, advanced stage and bone metastasis in prostate cancer. Oncogene 19:1288–1296. https://doi.org/10.1038/sj.onc.1203426

37. Knowles SM, Zettlitz KA, Tavaré R et al (2014) Quantitative ImmunoPET of prostate cancer xenografts with ^{89}Zr- and ^{124}I-Labeled Anti-PSCA A11 minibody. J Nucl Med 55:452–459. https://doi.org/10.2967/jnumed.113.120873
38. Knowles SM, Tavaré R, Zettlitz KA et al (2014) Applications of ImmunoPET: using ^{124}I-Anti-PSCA A11 minibody for imaging disease progression and response to therapy in mouse xenograft models of prostate cancer. Clin Cancer Res 20:6367–6378. https://doi.org/10.1158/1078-0432.CCR-14-1452
39. Tsai WK, Zettlitz KA, Tavaré R et al (2018) Dual-modality ImmunoPET/Fluorescence imaging of prostate cancer with an Anti-PSCA Cys-Minibody. Theranostics 8:5903–5914. https://doi.org/10.7150/thno.27679
40. Cacciamani GE, Shakir A, Tafuri A et al (2020) Best practices in near-infrared fluorescence imaging with indocyanine green (NIRF/ICG)-guided robotic urologic surgery: a systematic review-based expert consensus. World J Urol 38:883–896. https://doi.org/10.1007/s00345-019-02870-z
41. Zettlitz KA, Tsai W-TK, Knowles SM et al (2018) Dual-modality Immuno-PET and near-infrared fluorescence imaging of pancreatic cancer using an anti-prostate stem cell antigen cys-diabody. J Nucl Med 59:1398–1405. https://doi.org/10.2967/jnumed.117.207332
42. Tsai W-TK, Zettlitz KA, Dahlbom M et al (2020) Evaluation of [131I]I- and [177Lu]Lu-DTPA-A11 minibody for radioimmunotherapy in a preclinical model of PSCA-expressing prostate cancer. Mol Imag Biol 22:1380–1391. https://doi.org/10.1007/s11307-020-01518-4
43. Kramer CS, Dimitrakopoulou-Strauss A (2022) Immuno-imaging (PET/SPECT)–quo vadis? Molecules 27:3354. https://doi.org/10.3390/molecules27103354
44. Sterner RC, Sterner RM (2021) CAR-T cell therapy: current limitations and potential strategies. Blood Cancer J 11:69. https://doi.org/10.1038/s41408-021-00459-7
45. Adkins RN, MSN, ANP-C S, (2019) CAR T-cell therapy: adverse events and management. JADPRO 10. https://doi.org/10.6004/jadpro.2019.10.4.11
46. Koristka S, Kegler A, Bergmann R et al (2018) Engrafting human regulatory T cells with a flexible modular chimeric antigen receptor technology. J Autoimmun 90:116–131. https://doi.org/10.1016/j.jaut.2018.02.006
47. Arndt C, Bergmann R, Striese F et al (2022) Development and functional characterization of a versatile radio-/immunotheranostic tool for prostate cancer management. Cancers 14:1996. https://doi.org/10.3390/cancers14081996
48. Nijhout HF (2003) Development and evolution of adaptive polyphenisms. Evol Dev 5:9–18. https://doi.org/10.1046/j.1525-142X.2003.03003.x
49. Davies AH, Beltran H, Zoubeidi A (2018) Cellular plasticity and the neuroendocrine phenotype in prostate cancer. Nat Rev Urol 15:271–286. https://doi.org/10.1038/nrurol.2018.22
50. Conteduca V, Oromendia C, Eng KW et al (2019) Clinical features of neuroendocrine prostate cancer. Eur J Cancer 121:7–18. https://doi.org/10.1016/j.ejca.2019.08.011
51. Sharma SK, Pourat J, Abdel-Atti D et al (2017) Noninvasive interrogation of DLL3 expression in metastatic small cell lung cancer. Cancer Res 77:3931–3941. https://doi.org/10.1158/0008-5472.CAN-17-0299
52. Korsen JA, Kalidindi TM, Khitrov S et al (2022) Molecular imaging of neuroendocrine prostate cancer by targeting delta-like ligand 3. J Nucl Med Jnumed 121:263221. https://doi.org/10.2967/jnumed.121.263221
53. Mojtahedi A, Thamake S, Tworowska I et al (2014) The value of (68)Ga-DOTATATE PET/CT in diagnosis and management of neuroendocrine tumors compared to current FDA approved imaging modalities: a review of literature. Am J Nucl Med Mol Imag 4:426–434
54. Filippi L, Scopinaro F, Pelle G et al (2016) Molecular response assessed by 68Ga-DOTANOC and survival after 90Y microsphere therapy in patients with liver metastases from neuroendocrine tumours. Eur J Nucl Med Mol Imag 43:432–440. https://doi.org/10.1007/s00259-015-3178-3
55. Takahashi H, Shibuya M (2005) The vascular endothelial growth factor (VEGF)/VEGF receptor system and its role under physiological and pathological conditions. Clin Sci 109:227–241. https://doi.org/10.1042/CS20040370
56. Roberts E, Cossigny DAF, Quan GMY (2013) The role of vascular endothelial growth factor in metastatic prostate cancer to the skeleton. Prostate Cancer 2013:1–8. https://doi.org/10.1155/2013/418340
57. Li M, Jiang D, Barnhart TE et al (2019) Immuno-PET imaging of VEGFR-2 expression in prostate cancer with 89Zr-labeled ramucirumab. Am J Cancer Res 9:2037–2046
58. Persson BD, Schmitz NB, Santiago C et al (2010) Structure of the extracellular portion of CD46 provides insights into its interactions with complement proteins and pathogens. PLoS Pathog 6:e1001122. https://doi.org/10.1371/journal.ppat.1001122
59. Wang S, Li J, Hua J et al (2021) Molecular imaging of prostate cancer targeting CD46 using ImmunoPET. Clin Cancer Res 27:1305–1315. https://doi.org/10.1158/1078-0432.CCR-20-3310
60. Lenárt S, Lenárt P, Šmarda J et al (2020) Trop2: jack of all trades, master of none. Cancers 12:3328. https://doi.org/10.3390/cancers12113328
61. Hsu E-C, Rice MA, Bermudez A et al (2020) Trop2 is a driver of metastatic prostate cancer with neuroendocrine phenotype via PARP1. Proc Natl Acad Sci USA 117:2032–2042. https://doi.org/10.1073/pnas.1905384117
62. van Rij CM, Frielink C, Goldenberg DM et al (2015) Pretargeted ImmunoPET of prostate cancer with an anti-TROP-2 x anti-hsg bispecific antibody in mice with PC3 xenografts. Mol Imaging Biol 17:94–101. https://doi.org/10.1007/s11307-014-0772-x
63. Altai M, Membreno R, Cook B et al (2017) Pretargeted imaging and therapy. J Nucl Med 58:1553–1559. https://doi.org/10.2967/jnumed.117.189944
64. Oliveira MC, Correia JDG (2022) Clinical application of radioiodinated antibodies: where are we? Clin Transl Imag 10:123–162. https://doi.org/10.1007/s40336-021-00477-2
65. Zhang Z, Li D, Yun H et al (2022) CAR-T Cells in the treatment of urologic neoplasms: present and future. Front Oncol 12:915171. https://doi.org/10.3389/fonc.2022.915171